Solubility of cefuroxime axetil in supercritical CO2: measurement and modeling

Kanjana Ongkasin, Martial Sauceau, Yasmine Masmoudi, Jacques Fages, Elisabeth Badens

Solubility of cefuroxime axetil in supercritical CO_2: Measurement and modeling

K. Ongkasin [a], M. Sauceau [b], Y. Masmoudi [a], J. Fages [b], E. Badens [a,*]

[a] Aix Marseille Univ, CNRS, Centrale Marseille, M2P2, Marseille, France
[b] Centre RAPSODEE, IMT Mines Albi, CNRS, Université de Toulouse, 81013, Albi, France

HIGHLIGHTS

- Solubility of cefuroxime axetil in supercritical CO_2 was measured.
- Temperatures varying from 308 to 328 K and pressures from 8 to 25 MPa were studied.
- An analytical dynamic method was optimized for low amounts of drugs.
- Retrograde solubility behavior was observed.
- Solubility data were correlated with 4 semi-empirical density-based models.

GRAPHICAL ABSTRACT

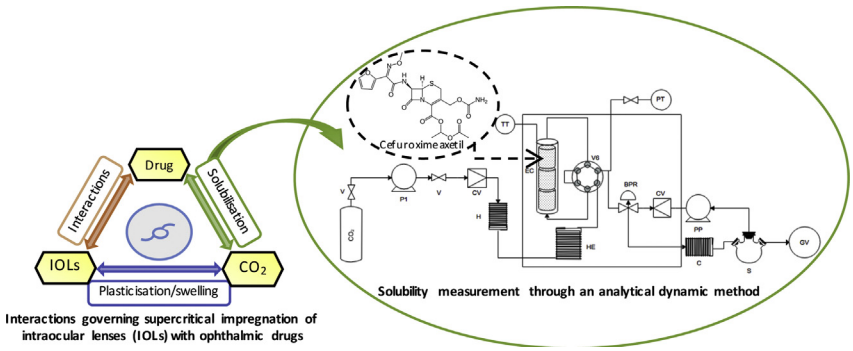

ABSTRACT

In this study, an analytical dynamic method was optimized for small amounts of drugs and used to measure the solubility of cefuroxime axetil in supercritical CO_2. After validating the experimental procedure with nimesulide, an active ingredient already studied in the literature, the solubility of cefuroxime axetil in supercritical CO_2 was measured at temperatures varying from 308 to 328 K and pressures ranging between 8 and 25 MPa. Experimental values varied between 2.2×10^{-7} and 11.24×10^{-6} (in mole fraction) and a retrograde solubility behavior was observed.

The solubility was correlated with semi-empirical density-based models: Kumar and Johnston, Mendez-Santiago and Teja, and Chrastil models. All three models successfully correlated the solubilities of cefuroxime axetil with an average deviation lower than 15%.

Keywords:
Supercritical carbon dioxide
Drug solubility measurement
Antibiotic
Density-based model

1. Introduction

Localized drug delivery systems, which allow drug delivery to a targeted tissue or organ, are fuelling a new generation of drug medication and leading, on one hand to minimal toxic side effects such as overdose or drug degradation and, on the other hand, to controlled drug release [1]. The development of such systems can benefit cataract surgery post-treatment if the active pharmaceutical ingredients (APIs), such as antibiotics or anti-inflammatory drugs, can be loaded into intraocular lenses (IOLs) thus making them a drug carrier [2]. Moreover, the use of loaded IOLs makes it possible to combine the two steps of surgery and postoperative medication in a single procedure without increasing the operation time.

Supercritical technology is an environmentally friendly route for drug impregnation which takes advantage of the specific properties of supercritical fluids (high density, low viscosity, diffusivity

* Corresponding author.
E-mail address: elisabeth.badens@univ-amu.fr (E. Badens).

Table 1
Chemical compounds.

Compound	Formula		Molar mass (g. mol^{-1})	Supplier
APIs				
Cefuroxime axetil	$C_{20}H_{22}N_4O_{10}S$	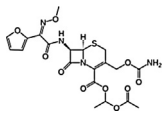	510.47	USP (France)
Nimesulide	$C_{13}H_{12}N_2O_5S$	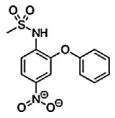	308.31	Sigma Aldrich (France)
Solvents				
Carbon dioxide	CO_2		44.01	Air Liquide (France)
Ethanol	C_2H_6O	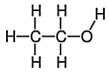	46.07	Sigma Aldrich (France)

higher than that of liquids, low interfacial tension, etc.). In particular, carbon dioxide (CO_2) presents very interesting properties such as non-flammability and non-toxicity. For medical and pharmaceutical processing, CO_2 notably presents the advantage of rather low critical coordinates, especially in terms of temperature (Pc = 7.38 MPa and Tc = 304.21 K). In ambient conditions of pressure and temperature, CO_2 is gaseous and therefore its separation at the end of the process is spontaneous upon depressurization. In addition, supercritical CO_2 ($SC-CO_2$) has biocidal properties, yet another advantage for medical applications [3]. One of the key parameters of supercritical impregnation is the partition of the drug between the supercritical fluid phase and the impregnated matrix.

The determination of the drug solute solubility in the fluid phase is therefore important in order to better control the supercritical impregnation process. Generally, the solubility of antibiotics or of anti-inflammatory drugs in CO_2 is very low. Indeed, it is the case of nimesulide [4–6], gatifloxacin [7], penicillin G [8], penicillin V [9], cefixime trihydrate [10], dexamethasone [11], azithromycin [12], erythromycin [12], clindamycin [12] and clarithromycin [12]. The values of their solubility vary between 10^{-7} and 10^{-5} (in mole fraction). The accuracy of the solubility measurement depends on the device and operational mode. Experimental techniques can be classified in synthetic and analytical methods depending on how the compositions of the equilibrium phases are determined [13,14]. In the synthetic methods, the determination of the phase composition is indirect without sampling, while in the analytical methods, the compositions are determined through analyses after sampling once the thermodynamic equilibrium is reached. In the analytical methods, it is possible to follow either a static or a dynamic method. In the static method, all the components are introduced in a closed cell, under stirring, so as to reach the thermodynamic equilibrium. In the dynamic method, one of the phases or the whole mixture flows through the system. In the latter case, the residence time of the flowing phase should be long enough to reach thermodynamic equilibrium.

Furthermore, the experimental results can be modeled following different approaches, including models based on equations of state (EoS). However, they require physicochemical properties such as critical temperatures and pressures, acentric factors or vapor pressures. Such properties are not available for many drug solutes and have to be estimated through group contribution methods. Therefore, the use of semi-empirical density-based models is a good alternative for modeling drug solute solubilities because of their simplicity [15].

With the aim of developing ophthalmic drug delivery systems dedicated to the prevention of postoperative endophthalmitis in cataract surgery, cefuroxime axetil, a second-generation cephalosporin antibiotic [16] was chosen as the antibiotic to be loaded into IOLs. This work aims to measure its solubility in supercritical CO_2 using an analytical dynamic method. A previously used set-up, based on an open circuit method allowing accurate measurements of low solute solubilities [17], was slightly modified in this study so as to require a low quantity of the drug. The experimental protocol was first validated using a solute with low solubility in $SC-CO_2$, nimesulide [4–6], a nonsteroidal anti-inflammatory drug. Then, the solubility of cefuroxime axetil was measured at a temperature varying from 308 to 328 K and at a pressure varying from 8 to 25 MPa. Finally, the experimental data were correlated using semi-empirical density-based models.

2. Materials and methods

2.1. Chemical compounds

Two active pharmaceutical ingredients were used within this study: nimesulide CAS: 51803-78-2 ($\geq$ 98% purity) and cefuroxime axetil CAS: 64544-07-6 (100% purity). Their formula, molar mass and their supplier are given in Table 1. The solvents employed were carbon dioxide (99.7% purity), ethanol ($\geq$ 99.8% purity) and ultrapure water.

2.2. Experiment

The solubility of drug solutes in supercritical CO_2 was measured using a continuous flow apparatus described previously [17] and illustrated in Fig. 1.

The set-up was mainly composed of an equilibrium cell (EC) withstanding pressures up to 50 MPa at temperatures up to 400 K. It contained three compartments (total volume of 4.5 cm^3) connected in series and fitted at their bottoms with stainless steel sintered disks and O rings. 350 mg of API and glass beads (2 mm diameter) were introduced into the equilibrium cell. This latter was then placed in a thermo-regulated oven. The glass beads were used so as to limit the quantity of APIs used while enhancing the dissolution phenomena by increasing the CO_2/API surface contact.

Upstream of the equilibrium cell, a feed circuit equipped with a CO_2 line and a co-solvent line allowed either a solubility measurement in pure supercritical CO_2 or in a CO_2/co-solvent mixture. In the present work, only solubilities in pure CO_2 were measured. It was introduced into the equilibrium cell by means of a syringe pump P1 (Isco, model 260 D) that could be operated in either constant-flow or constant-pressure mode for flow rates ranging from 0.1 μL min^{-1}

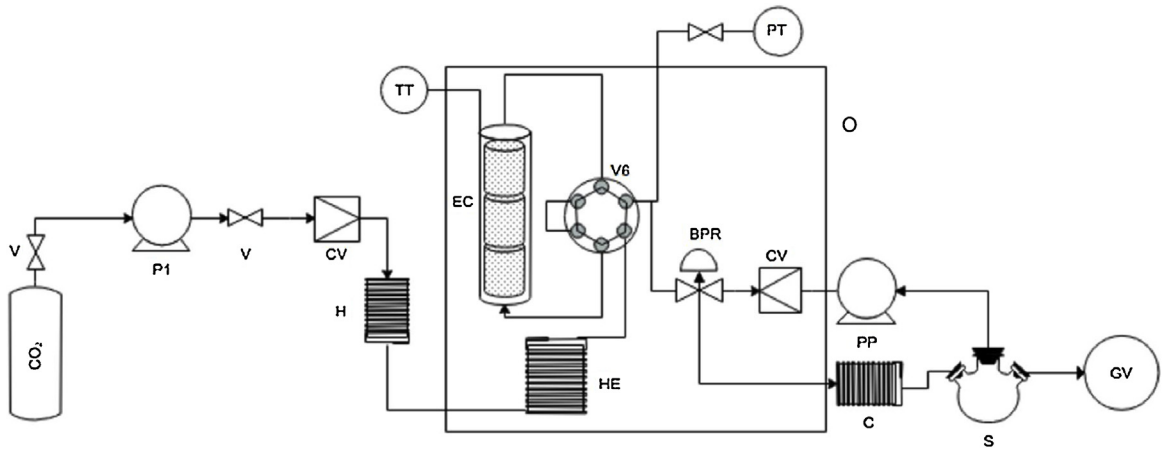

Fig. 1. Flow diagram of the set-up for solubility measurements V: 2 way valves; P1: high pressure pumps; M: mixer; CV: checking valve; H: heater; O: thermostated oven; HE: heat exchanger; V6: 6 way-2 position valve; EC: equilibrium cell; TT: temperature transducer; PT: pressure transducer; BPR: back pressure regulator; C: cooler; S: separator; PP: peristaltic pump; GV: gas volumeter.

to 90 mL min^{-1} and pressures up to 50 MPa. The feed line was also equipped with a heater (H) and a heat exchanger (HE) ensuring that the fluid phase would be set to the working temperature before entering the equilibrium cell. Downstream of the heat exchanger, a six-way, two-position high-pressure valve V6 was placed in the circuit to either direct the supercritical fluid to the cell or to bypass it.

Downstream of the equilibrium cell, a back-pressure regulator (BPR) allowed the regulation of the upstream pressure within 0.7% during the experiment, while the outlet of the BPR was at atmospheric pressure. To prevent solid precipitation and deposition resulting from the pressure drop as well as a potential resulting clogging, a recovering liquid solvent stream flowed at the outlet stream of the BPR. The liquid stream was cooled before entering a separator allowing the recovering solution to be collected (solvent/solute mixture) and the gaseous CO_2 to be vented out through a gas meter enabling the cumulative volume of gaseous CO_2 V_{CO2} (m^3) to be measured. At the end of each experimental run, the liquid solvent line was washed with fresh solvent to recover potential residual solute. The total volume of the recovering liquid phase V_L (m^3) was determined and its concentration in solute C^L_{solute} ($kg.m^{-3}$) measured using a UV–vis Spectrophotometer (Agilent Cary 8454 UV–vis). With these data, the solubility of the solute in the fluid phase (y) was calculated through Eq. (1):

$$y = \frac{n_{solute}}{n_{solute} + n_{CO2}} \tag{1}$$

where

$$n_{CO2} = \frac{V_{CO2} \times \rho_{CO2}}{M_{CO2}} \tag{2}$$

and

$$n_{solute} = \frac{C^L_{solute} \times V_L}{M_{solute}} \tag{3}$$

n (mol) is the number of mole, ρ ($kg.m^{-3}$) the density, and M ($kg.mol^{-1}$) the molar mass.

The first step in this work was to select the recovering solvent for UV–vis Spectroscopy analyses and to confirm the validity of the Beer-Lambert law for each compound studied. Ethanol was selected for nimesulide and ultrapure water for cefuroxime axetil. The calibration curves describing the evolution of the absorbance versus the solute concentration were determined by analyzing solutions with concentrations ranging between 0 and 50 μg.cm-3at 299 and 280 nm, respectively, for nimesulide and cefuroxime axetil. The concentration variation of each compound in thecorrespondingselected solvent was linear (c.f.

Fig. 2) with a coefficient of determination of 0.9995 and 0.9996, respectively.

In order to measure the solute solubility in the supercritical fluid phase, the CO_2 flow rate has to be tuned so as to ensure a sufficient residence time to reach saturation conditions of the solute in the fluid phase.

For the whole study, the solubility measurements were carried out at least in duplicate in each condition. The average values and the corresponding uncertainties were therefore indicated for the different conditions studied.

2.3. Semi-empirical correlations

Semi-empirical density-based models are widely used for determining the solubility of APIs [15,18]. In this work, four widely used density based correlations were selected to calculate the solubility of APIs: Kumar and Johnston [19], Chrastil [20] and Mendez-Santiago and Teja [21] models.

In the Kumar and Johnston models, the solubility of APIs in the supercritical fluid phase in mole fraction (y) varies linearly in log-linear coordinates or log-log plot of the SC−CO_2 density (Eq. (4) and Eq. (5), respectively). The slope is related to the solvent isothermal compressibility and the partial molar volume of the solute present at infinite dilution in the supercritical fluid phase [19].

$$\ln(y) = a_1 + b_1 \rho \tag{4}$$

$$\ln(y) = a_2 + b_2 \ln(\rho) \tag{5}$$

where ρ ($kg\,m^{-3}$) is the density of the fluid phase and a_1, b_1, a_2, b_2 are adjusted to solubility experimental data.

The second semi-empirical model used in this work was suggested by Chrastil [20] (Eq. (6)) and is based on the hypothesis that one molecule of a solute associates with k molecules of the supercritical solvent to form a solvato complex in equilibrium with the system. The definition of the equilibrium constant through thermodynamic considerations leads to the following expression for the solubility:

$$\ln(y) = a_3 + k\ln(\rho) + \frac{c_3}{T} \tag{6}$$

k is the association number, c_3 is dependent on both solvation and vaporization enthalpies of the solute, and a_3 is dependent on the molecular weights of the species.

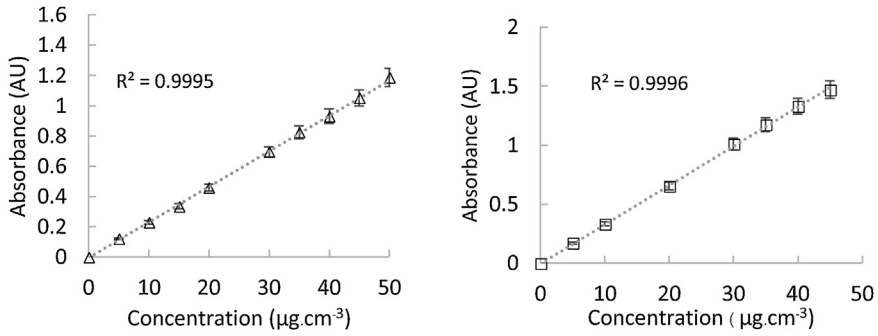

Fig. 2. Calibration curve of Δ) nimesulide in ethanol and □) cefuroxime axetil in ultrapure water.

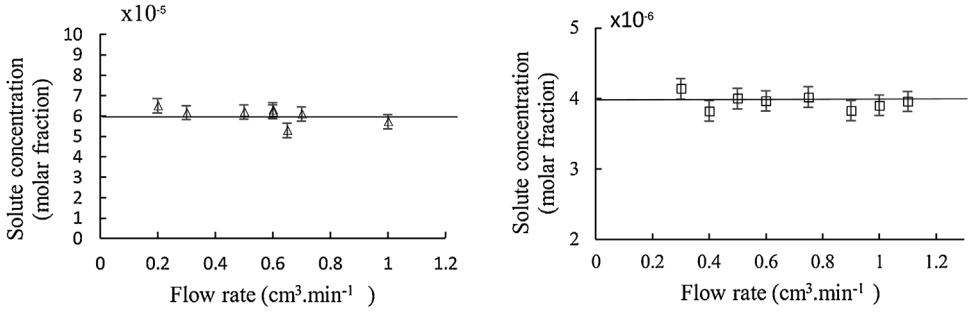

Fig. 3. Evolution of solute concentration in pure CO_2 with CO_2 flowrate Δ) nimesulide (at 313 K and 19 MPa) and □) cefuroxime axetil (at 308 K and 16.5 MPa).

The third model was suggested by Mendez-Santiago and Teja [21] (Eq. (7)) who derived a relation from the theory of dilute solution near the critical point of the solvent by simplified expressions of Harvey [22].

$$T \ln(yP) = a_4 + b_4 \rho + c_4 T \tag{7}$$

T is the temperature of the supercritical phase and a_4, b_4, c_4 are adjusted to solubility experimental data.

For each model, the average absolute relative deviation (AARD) between correlated and experimental data were calculated according to Eq. (8) and used as the index to check the accuracy of the modeling systems.

$$\text{AARD}(\%) = \frac{100}{N}\sum_{i=1}^{N}\frac{\left|y_{cal} - y_{exp}\right|}{y_{exp}} \tag{8}$$

y_{cal} is the solubility derived from the model, y_{exp} the experimental solubility and N the number of data points.

3. Results and discussions

3.1. CO_2 flow rate selection and repeatability

In order to measure the solute solubility in SC−CO_2, the residence time of CO_2 in the equilibrium cell should be sufficient to reach the saturation conditions of the solute in the fluid phase. For that purpose, the experiment was repeated while gradually increasing the CO_2 flowrate. A constant concentration at different flowrates indicates saturation of solute in the supercritical phase. If the concentration decreases with a further increase in CO_2 flowrate, this indicates that the residence time is becoming too short to ensure saturation conditions.

At a constant CO_2 flowrate, the solubility uncertainty depends on the duration of the experiment: the longer the duration, the higher the quantity of the recovered solute and the more accurate the solubility value. Therefore, the flow rate should be selected while respecting the saturation conditions without imposing an excessively long experiment. The solubility measurements were carried out at least in duplicate in each condition.

Fig. 3 shows a stable concentration of nimesulide in supercritical CO_2 at 313 K and 19 MPa in flowrate range between 0.2 and 1.1 $cm^3.min^{-1}$. A stable concentration cefuroxime axetil in supercritical CO_2 at 308 K and 16.5 MPa was also observed in the CO_2 flowrate range of 0.3 to 1.2 $cm^3.min^{-1}$. The CO_2 flow rate was thus fixed at 0.65 $cm^3.min^{-1}$ for each compound and the solute recovering step was set to about 35 min to obtain measured concentrations in the calibration range of the spectrophotometer.

3.2. Nimesulide solubility measurements and procedure validation

The validity of the experimental procedure was tested by measuring nimesulide solubility in pure supercritical CO_2 since some solubility data of this nonsteroidal anti-inflammatory drug in SC−CO_2 at 313 K and for different pressures are available in the literature. Caputo et al. [4] and Abdelli [6] measured nimesulide solubility by using a static method while Macnaughton et al. [5] used a dynamic method. Its solubility in SC−CO_2 varied between 1.95×10^{-5} and 7.42×10^{-5} (in mole fraction) for pressures ranging between 13 and 22 MPa at 313 K.

Comparison of solubility data determined in this study with those reported from the literature is illustrated in

Fig. 4 and shows a rather good agreement between the results. The results validate the developed experimental protocol based on the analytical dynamic method while using a small quantity of solute (as low as 350 mg).

3.3. Cefuroxime axetil solubility measurements

The solubility of cefuroxime axetil in supercritical CO_2 was experimentally measured using the validated dynamic method at pressures ranging between 8 and 25 MPa in isothermal conditions (308, 318 and 328 K). The measured solubilities data are presented in Table 2 and graphically illustrated in

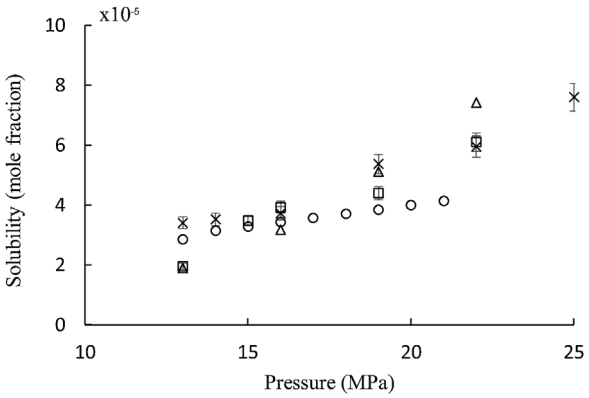

Fig. 4. Comparison of solubility data of nimesulide in SC–CO_2 at 313 K; o, Caputo [4]; Δ, Macnaughton [5]; □, Abdelli [6]; ×, Present work.

Table 2
Cefuroxime axetil solubility in supercritical CO_2 at 308, 318 and 328 K.

Temperature (K)	Pressure (MPa)	ρ_{CO_2} (kg. m^{-3})[a]	$10^6 \times y$
308	8.0	419.09	0.51 ± 0.03
	10.0	712.81	0.72 ± 0.04
	12.0	767.05	2.06 ± 0.12
	14.0	801.41	1.80 ± 0.07
	16.5	832.78	3.91 ± 0.23
	20.0	865.73	6.19 ± 0.37
	25.0	901.23	11.24 ± 0.67
318	8.0	241.05	0.22 ± 0.01
	12.0	657.74	0.83 ± 0.03
	14.0	720.47	1.35 ± 0.08
	16.5	768.02	3.23 ± 0.19
	20.0	812.69	5.14 ± 0.31
	25.0	857.14	9.70 ± 0.58
328	8.0	203.64	0.27 ± 0.02
	12.0	504.51	0.50 ± 0.03
	14.0	618.45	0.67 ± 0.04
	16.5	692.97	1.75 ± 0.10
	20.0	754.61	3.50 ± 0.21
	25.0	810.65	7.76 ± 0.45

[a] Density data from NIST chemistry webbook using Span and Wagner model [23].

Fig. 5 indicating that the solubility of cefuroxime axetil in SC–CO_2 varied from 2.2×10^{-7} to 11.24×10^{-6} (mole fraction) in the experimental conditions studied. The temperature and the pressure were measured with the following uncertainties: ± 0.1 °C and ± 0.05 MPa.

As shown in Fig. 5, in isothermal conditions, cefuroxime axetil solubility increases as the pressure increases which is coherent with the corresponding rise in CO_2 density.

In the range of pressure tested, the solubility decreases when the temperature increases indicating retrograde solubility behavior [24]. The variation of solubility as a function of temperature at isobaric conditions results in two competing effects. On one hand, increasing the temperature induces a decrease in CO_2 density thereby limiting interactions between solute and CO_2 molecules which tends to reduce solubility. On the other hand, an increase in the solute vapor pressure with a temperature rise enhances solubility. In the retrograde zone, the effect on the supercritical phase density prevails while at higher pressures (as for pressures lower than the lower limit of the retrograde zone) the effect of vapor pressure becomes predominant resulting in an increase in solubility when the temperature increases. In our experimental conditions, the crossover pressure corresponding to the upper limit of the retrograde zone is therefore higher than 25 MPa.

The measured solubility data were then correlated using 4 semi-empirical density-based equations corresponding to the Kumar and Johnston (Eqs. (4) and (5)), Chrastil (Eq. (6)), and Mendez-Santiago and Teja (Eq. (7)) models. In the four correlations, the density of the fluid phase is required. As the solubility of cefuroxime axetil in CO_2 is very low (between 2.2×10^{-7} and 11.24×10^{-6} in the tested experimental conditions), its influence on the fluid phase density was neglected and the density of the saturated fluid phase was thus considered equal to that of pure CO_2. The modeling work was focused on the operating range corresponding to densities higher than 500 kg.m^{-3}. This was done because for densities lower than 500 kg.m^{-3}, the lowest solubilities were measured and the largest uncertainties were found.

Results of the modeling work are illustrated in Table 3 and Fig. 6. The fitting of the experimental solubility data with the three semi-empirical models leads to an average relative deviation ranging between 2.1 and 15.1% indicating a satisfactory regression of the results and thus a possible prediction of cefuroxime axetil solubility at temperature and pressure in the investigated regions using the correlation parameters estimated within this study.

As illustrated in Table 3 and Fig. 6, the results of the Kumar and Johnston model show a linear variation of cefuroxime axetil solubility with the fluid phase density in either log-linear (Eq. (4)) and log-log (Eq. (5)) coordinates at each isotherm with respective average relative deviations (AARD) between 2.1 to 12.7% and 4.1 to 14.5%.

The experimental data were also regressed using the Chrastil correlation in the different isothermal conditions studied. As illustrated in Table 3, a slight decrease in the association number k is observed when the temperature increases which is coherent with a higher association at lower temperature. Nevertheless, as the values of k were close for the different temperatures, the Chrastil model was correlated with the overall experimental results allow-

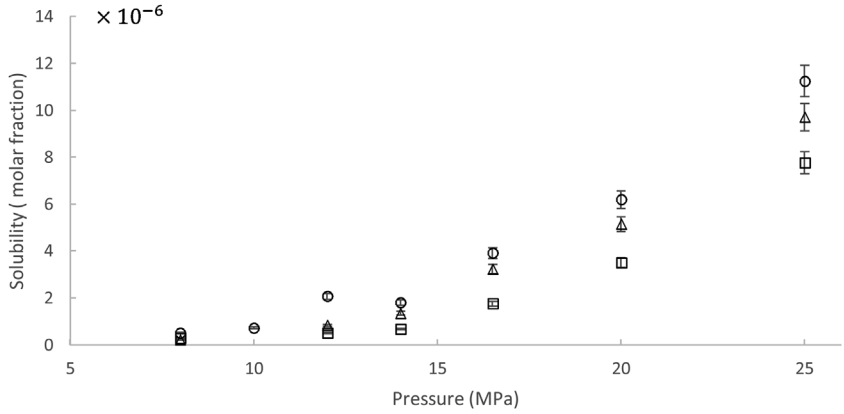

Fig. 5. Solubility of cefuroxime axetil in supercritical CO_2 at different temperatures; (o) 308 K; (Δ) 318 K; (□) 328 K.

Table 3
Correlation of cefuroxime axetil solubility in SC–CO_2 with the semi-empirical density-based correlations.

Models	Correlations	T(K)	Number of points	model parameters			
				a_1	b_1		AARD (%)
Kumar and Johnston	Eq. (4)	308	6	1.40×10^{-2}	−24.14		12.7
		318	5	1.27×10^{-2}	−22.45		9.3
		328	4	1.26×10^{-2}	−22.03		2.1
				a_2	b_2		AARD (%)
	Eq. (5)	308	6	−88.07	11.25		14.5
		318	5	−75.83	9.50		11.1
		328	4	−72.49	9.06		4.1
				a_3	k	c_3	AARD (%)
Chrastil	Eq. (6)	308	6	−88.07	11.25	–	14.5
		318	5	−75.83	9.50	–	11.1
		328	4	−72.49	9.06	–	4.1
		overall	15	−61.92	9.77	−5002.03	12.7
				a_4	b_4	c_4	AARD (%)
Mendez-Santiago and Teja	Eq. (7)	308	6	5.83	−7819.73	–	15.1
		318	5	5.20	−7135.73	–	11.2
		328	4	5.20	−7037.66	–	3.6
		overall	15	5.38	−11825.79	14.23	12.0

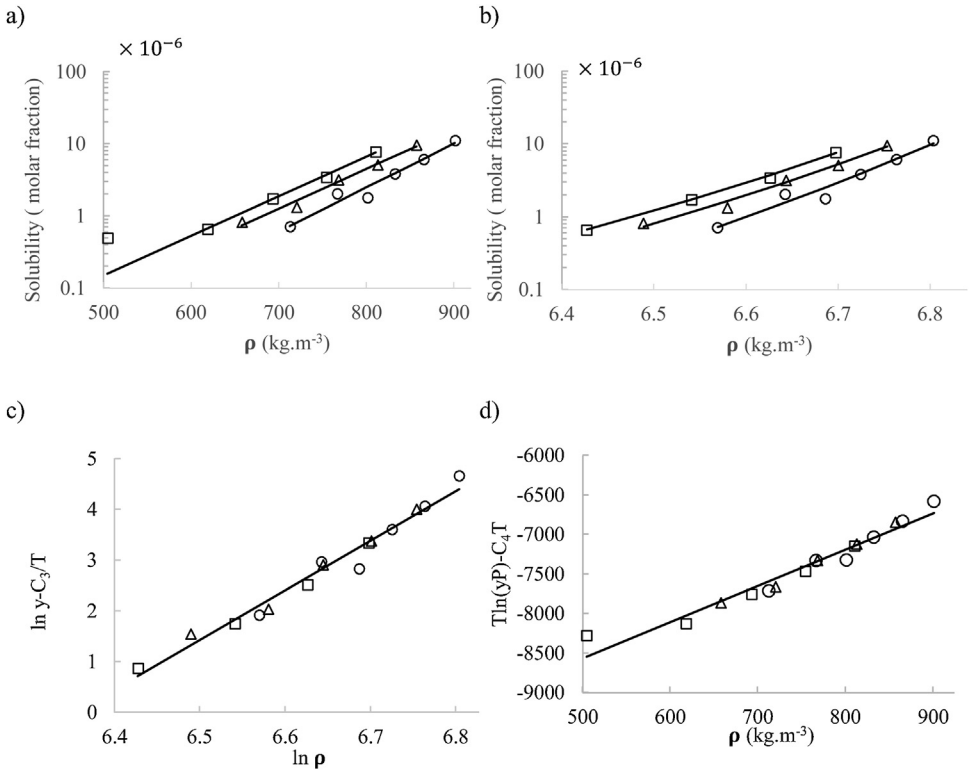

Fig. 6. Correlation cefuroxime axetil solubility in SC–CO_2 with the semi-empirical density-based correlations at different temperatures; o, 308 K; Δ, 318 K; □, 328 K (a) Kumar correlation in semi-log coordinates (Eq. (4)),(b) Kumar correlation semi-log coordinates (Eq. (5)),(c) Chrastil correlation (Eq. (6)),(d) Mendez-Santiago and Teja correlation (Eq. (7)).

ing the average values of the model parameters a_3, k, and b_3 to be adjusted for the three temperatures. As illustrated by the Chrastil correlation in Fig. 6c, the variation of $\ln(y) - \frac{c_3}{T}$ is linear as a function of ln(ρ) with an average relative deviation (AARD) of 12.7% indicating a good correlation of the experimental solubility measurements with only one model regardless of the pressure and the temperature.

Solubility data were also regressed with the Mendez-Santiago and Teja model. As for the Chrastil model, close values of the model constants a_4 and b_4 were obtained for the different temperatures studied. The model was therefore used to correlate the overall experimental results. As illustrated in Fig. 6d, the variation of T ln(y P)-c_4T with the density of the fluid phase is linear with an average relative deviation (AARD) of 12.0% indicating a satisfactory correlation of the experimental results independently of the pressure and the temperature conditions.

Finally, all the modeled data are grouped on the graph shown on Fig. 7.

4. Conclusion

Solubility of cefuroxime axetil in pure supercritical CO_2 was measured through an analytical dynamic method at temperatures varying from 308 to 328 K and pressures ranging between 8 and 25 MPa. The experimental procedure was improved in comparison to a previously validated protocol by introducing glass beads into the equilibrium cell so as to limit the quantity of API used during the experiment. The method was first validated by measuring the

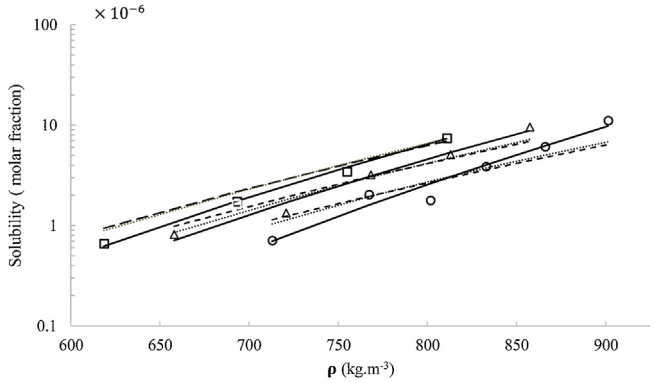

Fig. 7. Cefuroxime axetil solubility in SC−CO_2 with the semi-empirical density-based correlations at different temperatures; o, 308 K; Δ, 318 K; □, 328 K (—) Kumar correlation, (—) Chrastil correlation, (. . .) Mendez-Santiago and Teja correlation.

solubility of nimesulide, an API already studied in the literature. The solubility of cefuroxime axetil in supercritical CO_2 was then measured and varied between 2.2×10^{-7} and 11.24×10^{-6} (in mole fraction) in the operating conditions studied. A retrograde solubility behavior was observed in the conditions studied.

Four semi-empirical density-based models were used to correlate the experimental solubilities for densities higher than 500 $kg.m^{-3}$. The average deviation was lower than 15% for all the models, indicating a possible prediction of cefuroxime axetil solubility at temperature and pressure in the investigated regions using the correlation parameters evaluated within this study. Compared to the Kumar and Johnston model that allows the adjustment of the experimental data in each isothermal condition, by using the Chrastil and Mendez-Santiago and Teja models, it was possible to correlate the experimental results using only one model with average parameters in the experimental range of pressures and temperatures studied. Modeling of cefuroxime axetil solubility in SC−CO_2 at low pressure needs to be further improved.

The measured drug solubility values can be useful for further drug impregnation experiments. The targeted application is the supercritical impregnation of cefuroxime axetil into intraocular lenses. The drug solubility values estimated in this present work will allow the estimation of drug partition coefficient between the fluid phase and the impregnation support, provided that drug loadings are known. Even if the solubility values are low, the drug impregnation rate can be significant [25] since the main parameter controlling supercritical impregnation is the partition coefficient of the drug between the fluid phase and the impregnated matrix. Moreover, the targeted drug impregnation rate can be low depending on the application such as for ophthalmic devices. For the impregnation of an antibiotic drug into intraocular lenses, a loading of about a few micrograms of drug per milligram of polymeric lens can be sufficient depending on the desired effect.

Acknowledgements

The authors would like to thank the Thai Ministry of Science and Technology for Kanjana Ongkasin's PhD grant in the framework of the Royal Thai Government Scholarship.

References

[1] Y. Perrie, T. Rades, Pharmaceutics: Drug Delivery and Targeting, Pharmaceutical Press, London, 2010.
[2] J.L. Bourges, C. Bloquel, A. Thomas, F. Froussart, A. Bochot, F. Azan, R. Gurny, D. BenEzra, F. Behar-Cohen, Intraocular implants for extended drug delivery: therapeutic applications, Adv. Drug Deliv. Rev. 58 (2006) 1182–1202, http://dx.doi.org/10.1016/j.addr.2006.07.026.
[3] I. Rehman, J. Darr, A. Moshaverinia, Supercritical fluid processing, in: G. Wnek, G. Bowlin (Eds.), Encycl. Biomater. Biomed. Eng. Second Ed. - Four Vol. Set, CRC Press, 2008, pp. 2522–2530, http://dx.doi.org/10.1201/b18990-243 (accessed July 17, 2018).
[4] G. Caputo, M. Scognamiglio, I. De Marco, Nimesulide adsorbed on silica aerogel using supercritical carbon dioxide, Chem. Eng. Res. Des. 90 (2012) 1082–1089, http://dx.doi.org/10.1016/j.cherd.2011.11.011.
[5] S.J. Macnaughton, I. Kikic, N.R. Foster, P. Alessi, A. Cortesi, I. Colombo, Solubility of anti-inflammatory drugs in supercritical carbon dioxide, J. Chem. Eng. Data 41 (1996) 1083–1086, http://dx.doi.org/10.1021/je960103q.
[6] S. Abdelli, Cristallisation Par Procédé Supercritique Anti-solvant (SAS) : Influence Des Conditions Opératoires Sur Le Polymorphisme Des Cristaux," PhD Thesis, Aix-marseille Université, PhD Thesis, Aix-Marseille université, 2017 http://www.theses.fr/2017AIXM0362.
[7] K. Shi, L. Feng, L. He, H. Li, Solubility determination and correlation of gatifloxacin, enrofloxacin, and ciprofloxacin in supercritical CO_2, J. Chem. Eng. Data 62 (2017) 4235–4243, http://dx.doi.org/10.1021/acs.jced.7b00601.
[8] M. Gordillo, M. Blanco, A. Molero, E. Martinez de la Ossa, Solubility of the antibiotic Penicillin G in supercritical carbon dioxide, J. Supercrit. Fluids 15 (1999) 183–190, http://dx.doi.org/10.1016/S0896-8446(99)00008-X.
[9] M. Ko, V. Shah, P.R. Bienkowski, H.D. Cochran, Solubility of the antibiotic penicillin V in supercritical CO2, J. Supercrit. Fluids 4 (1991) 32–39, http://dx.doi.org/10.1016/0896-8446(91)90028-5.
[10] M. Khamda, M.H. Hosseini, M. Rezaee, Measurement and correlation solubility of cefixime trihydrate and oxymetholone in supercritical carbon dioxide (CO2), J. Supercrit. Fluids 73 (2013) 130–137, http://dx.doi.org/10.1016/j.supflu.2012.09.006.
[11] R.B. Chim, M.B.C. de Matos, M.E.M. Braga, A.M.A. Dias, H.C. de Sousa, Solubility of dexamethasone in supercritical carbon dioxide, J. Chem. Eng. Data 57 (2012) 3756–3760, http://dx.doi.org/10.1021/je301065f.
[12] H. Asiabi, Y. Yamini, F. Latifeh, A. Vatanara, Solubilities of four macrolide antibiotics in supercritical carbon dioxide and their correlations using semi-empirical models, J. Supercrit. Fluids 104 (2015) 62–69, http://dx.doi.org/10.1016/j.supflu.2015.05.018.
[13] R.E. Fornari, P. Alessi, I. Kikic, High pressure fluid phase equilibria: experimental methods and systems investigated (1978–1987), Fluid Phase Equilib. 57 (1990) 1–33, http://dx.doi.org/10.1016/0378-3812(90)80010-9.
[14] J.M.S. Fonseca, R. Dohrn, S. Peper, High-pressure fluid-phase equilibria: experimental methods and systems investigated (2005–2008), Fluid Phase Equilib. 300 (2011) 1–69, http://dx.doi.org/10.1016/j.fluid.2010.09.017.
[15] A. Belghait, C. Si-Moussa, M. Laidi, S. Hanini, Semi-empirical correlation of solid solute solubility in supercritical carbon dioxide: comparative study and proposition of a novel density-based model, Comptes Rendus Chim. 21 (2018) 494–513, http://dx.doi.org/10.1016/j.crci.2018.02.006.
[16] P. Dellamonica, Cefuroxime axetil, Int. J. Antimicrob. Agents 4 (1994) 23–36, http://dx.doi.org/10.1016/0924-8579(94)90061-2.
[17] M. Sauceau, J. Fages, J.-J. Letourneau, D. Richon, A novel apparatus for accurate measurements of solid solubilities in supercritical phases, Ind. Eng. Chem. Res. 39 (2000) 4609–4614, http://dx.doi.org/10.1021/ie000181d.
[18] M. Sauceau, J.-J. Letourneau, D. Richon, J. Fages, Enhanced density-based models for solid compound solubilities in supercritical carbon dioxide with cosolvents, Fluid Phase Equilib. 208 (2003) 99–113, http://dx.doi.org/10.1016/S0378-3812(03)00005-0.
[19] S.K. Kumar, K.P. Johnston, Modeling the solubility of solids in supercritical fluids with density as the independent variable, J. Supercrit. Fluids 1 (1988) 15–22, http://dx.doi.org/10.1016/0896-8446(88)90005-8.
[20] J. Chrastil, Solubility of solids and liquids in supercritical gases, J. Phys. Chem. 86 (1982) 3016–3021, http://dx.doi.org/10.1021/j100212a041.
[21] J. Méndez-Santiago, A.S. Teja, The solubility of solids in supercritical fluids, Fluid Phase Equilib. 158–160 (1999) 501–510, http://dx.doi.org/10.1016/S0378-3812(99)00154-5.
[22] A.H. Harvey, Supercritical solubility of solids from near-critical dilute-mixture theory, J. Phys. Chem. 94 (1990) 8403–8406, http://dx.doi.org/10.1021/j100385a009.
[23] R. Span, W. Wagner, A new equation of state for carbon dioxide covering the fluid region from the triple-Point temperature to 1100 K at pressures up to 800 MPa, J. Phys. Chem. Ref. Data 25 (1996) 1509–1596, http://dx.doi.org/10.1063/1.555991.
[24] E. Stahl, K.W. Quirin, Dense gas extraction on a laboratory scale: a survey of some recent results, Fluid Phase Equilib. 10 (1983) 269–278, http://dx.doi.org/10.1016/0378-3812(83)80040-5.
[25] A. Bouledjouidja, Y. Masmoudi, M. Sergent, E. Badens, Effect of operational conditions on the supercritical carbon dioxide impregnation of anti-inflammatory and antibiotic drugs in rigid commercial intraocular lenses, J. Supercrit. Fluids 130 (2017) 63–75, http://dx.doi.org/10.1016/j.supflu.2017.07.015.